The Mechanism of Amyloid Spherulite Formation by Bovine Insulin

M. R. H. Krebs, E. H. C. Bromley, S. S. Rogers, and A. M. Donald
Biological and Soft Systems, Cavendish Laboratory, University of Cambridge, United Kingdom

ABSTRACT The formation of amyloid-containing spherulite-like structures has been observed in some instances of amyloid diseases, as well as in amyloid fibril-containing solutions in vitro. In this article we describe the structure and kinetics of bovine insulin amyloid fibril spherulites formed in the presence and absence of different salts and at different salt concentrations. The general spherulite structure consists of radially oriented amyloid fibrils, as shown by optical microscopy and environmental scanning electron microscopy. In the center of each spherulite, a ''core'' of less regularly oriented material is observed, whose size decreases when the spherulites are formed in the presence of increasing concentrations of NaCl. Similarly, amyloid fibrils form faster in the presence of NaCl than in its absence. A smaller enhancement of the rate of formation with salt concentration is observed for spherulites. These data suggest that both amyloid fibril formation and random aggregation occur concurrently under the conditions tested. Changes in their relative rates result in the different-sized cores observed in the spherulites. This mechanism can be likened to that leading to the formation of spherulites of polyethylene, in agreement with observations that polypeptide chains under partially denaturing conditions can exhibit behavior not dissimilar to that of synthetic polymers.

INTRODUCTION

Spherulites are most commonly associated with synthetic polymers (Bassett, 2003; Magill, 2001). Characteristic of spherulites are the regular arrangement of polymer chains within them, resulting in the appearance of a Maltese cross extinction pattern when the spherulites are studied under a polarized light microscope. In the case of polyethylene (PE), the spherulite structure is well-documented after 40 years of research, as reviewed recently by Bassett (2003). One mechanism of PE spherulite formation suggests that the PE chains fold to form lamellae. Although in principle regularly shaped, their fold surfaces are not flat: the PE chains often form loops on the surface or are incompletely incorporated into the lamellae. Thus, when the lamellae form and attempt to line up as a polymer melt is cooled, rather than being parallel they lie at an angle that varies with supercooling and the lamella dimensions, but is commonly $\sim 20°$. The space in between these major lamellae is filled in by the formation of minor lamellae at similar angles, and polymer chains that have not crystallized at all. Ultimately, spherical structures are formed in which the lamellae lie in a radial orientation; consequently the polymer chain is in a tangential arrangement (Bassett, 2003). In a different model, the formation of lamellae is nucleated by already existing lamellae, resulting in the formation of lamellae at various angles and, ultimately, a spherical structure (Gránásy et al., 2004; Magill, 2001).

Many other systems have been found to form spherulitic structures, such as lyotropic liquid crystal systems (Donald and Windle, 1992), synthetic cellulose (Kobayashi et al., 2000), chitin and chitosan (Murray and Neville, 1997, 1998), amylose (Ring et al., 1987), sodium adducts of DNA (Rill, 1986), proteins such as lysozyme (Chow et al., 2002; Tanaka et al., 1997) and carboxypeptidase (Coleman et al., 1960) under crystallization conditions, tubules from bacteriochlorophyll protein (Olson, 1970), and fibers formed from haemoglobin-S, a mutational variant of the human protein leading to sickle cell anemia (Hofrichter, 1986). Surprisingly, spherulitic deposits have also been observed in vivo associated with mammary tumors in dogs (Taniyama et al., 2000; Vos and Gruys, 1985) and with amyloid tumors, localized nodular masses of amyloid deposits not linked to systemic amyloidosis, observed in the jejunum, part of the small intestine (Acebo et al., 1999). Other amyloid diseases have similarly been observed to occasionally contain spherulitic structures in the corpora amylacea or amyloid plaques. These include Creutzfeld-Jacob disease (Manuelidis et al., 1997), a rat model of Alzheimer's disease (Snow et al., 1994), and Alzheimer's and Gerstmann-Sträusler-Scheinker diseases and Down's syndrome (Jin et al., 2003). As in all amyloid diseases, the plaques contain many different components, including amyloid fibrils (Sipe, 1992). It is not obvious how often spherulitic deposits are found in amyloid plaques, as not all references refer to the spherulitic deposits by name or show images of the affected areas by polarized light microscopy.

Amyloid fibrils are large polymeric assemblies composed of multiple copies of a single protein. The protein involved in the amyloid fibrils is specific for each disease. The fibrils tend to be long (>1 μm) and unbranched, with diameters typically between 6 and 12 nm (Sunde and Blake, 1997). All amyloid fibrils possess a common underlying structure irrespective of the polypeptide precursor, and all give rise to a ''cross-β'' x-ray fiber diffraction pattern indicating that the β-strands making up the fibril backbone lie perpendicular to the fibril

Submitted August 27, 2004, and accepted for publication December 2, 2004.

Address reprint requests to M. R. H. Krebs, BSS, Cavendish Laboratory, University of Cambridge, Madingley Rd., Cambridge CB3 0HE, UK. Tel.: 44-1223-765-695; Fax: 44-1223-337-000; E-mail: mrhk2@cam.ac.uk.

© 2005 by the Biophysical Society

0006-3495/05/03/2013/09 $2.00

doi: 10.1529/biophysj.104.051896

axis (Sunde and Blake, 1997). Similar structures can be formed in vitro from a variety of peptides and proteins not associated with disease, suggesting that the ability to form amyloid fibrils is a common and perhaps generic property of polypeptide chains (Dobson, 2003; MacPhee and Dobson, 2000).

Like their disease-associated counterparts, several amyloid fibril-forming polypeptide sequences have been observed to form spherulites in vitro: a pathogenic immunoglobulin light chain (Raffen et al., 1999), several synthetic peptides (Aggeli et al., 2003), including a helix-turn-helix peptide (Fezoui et al., 2000), the nonpathogenic protein α-L-iduronidase (Ruth et al., 2000), a synthetic peptide derived from the β-sheet domain of platelet factor-4 (Lockwood et al., 2002), the 40-residue Aβ peptide, implicated in Alzheimer's disease, where the spherical aggregates were termed ''beta-amy balls'' (Westlind-Danielsson and Arnerup, 2001), and β-lactoglobulin (Bromley et al., 2004; Sagis et al., 2002).

Bovine insulin is a small protein whose capacity to form fibrillar structures and ''spherites'' has been known for almost 60 years (Waugh, 1946). The fibrillar structures formed have been confirmed to be amyloid fibrils (Bouchard et al., 2000; Nielsen et al., 2001b). In a recent article, we described the structure of bovine insulin amyloid fibril spherulites formed in the absence of salt (Krebs et al., 2004) and found that the ''spherites'' observed by Waugh in 1946 are identical in structure to the wide range of spherulites described above. In this article, the structures of spherulites formed under different conditions are described and compared using a variety of microscopic techniques. Furthermore, the mechanism of formation of the spherulites is explored by following the formation of amyloid fibrils and spherulites using fluorescence and birefringence assays.

EXPERIMENTAL PROCEDURE

Proteins and solutions

Bovine insulin and all other chemicals were of analytical grade or better, and were obtained from the Sigma-Aldrich Company (Gillingham, UK) and used without further purification. Protein solutions were made up by weighing out the required amounts of salt and insulin and dissolving the dry powders in MilliQ water adjusted to pH 2.0 with HCl. The pH was then checked and, if necessary, adjusted with 1-M solutions of HCl or NaOH. It was found using ultraviolet (UV) absorption at 280 nm that insulin concentrations obtained by this method, ranging from 1 to 10 mM, were accurate to within 10%. To induce the formation of fibrils and spherulites, solutions in glass vials were placed in a heating block without stirring at 65°C or 55°C for differing amounts of time up to 24 h. The start of the incubation time was taken when the solution reached the desired temperature. After incubating 1-mM insulin solutions in the presence or absence of salt at these temperatures for 24 h, spherulite solutions had formed. The number of spherulites in solution was increased up to 10-fold by centrifugation of solutions containing spherulites and removal of the supernatant.

Optical and confocal microscopy

After incubation, aliquots of insulin solutions were removed from the glass vials using Pasteur pipettes and put onto microscope slides. The slides were immediately studied using a Zeiss Axioplan optical microscope (Carl Zeiss, Welwyn Garden City, UK) without coverslips and at objective lens magnifications of up to 50×. Polarizer and analyzer were in a fixed position (east-west and north-south on the images as shown). A 551-nm retardation plate was inserted at 45° to the polarizers, with the fast optical axis northwest-southeast. Digital images were taken and scale bars were obtained by taking images of a calibration slide with the same settings on the microscope and the digital camera. At least 30 measurements were made from digital images from several different samples formed under the different conditions to measure spherulite ''core'' sizes. Spherulite sizes were measured from further digital images taken from several aliquots from each of at least six different solutions incubated in the presence or absence of salt for 24 h.

Confocal microscopy was performed on a Zeiss LSM750 microscope (Carl Zeiss) at objective lens magnifications of up to 40×. For fluorescence measurements, thioflavin-T was added to spherulite solutions and excited using the 458-nm line of an argon ion laser. Simultaneously, transmission images were obtained with crossed polarizers in place using the 633-nm line of a HeNe laser.

Environmental scanning electron microscopy

Aliquots of incubated solutions were taken and placed on aluminium stubs inside the microscope chamber of an FEI, 2010 environmental scanning electron microscopy (ESEM; FEI Company, Hillsboro, OR). The samples were left to equilibrate at 2°C (temperature controlled by a Peltier-device under the sample stub). A few drops of distilled and deionized water were placed around the sample, the chamber sealed and evacuated initially to ~6 Torr. The chamber was flooded repeatedly with water vapor and the pressure subsequently reduced slowly to ~5 Torr. Further decreases in pressure led to evaporation of the water and drying of the samples; conversely, increasing the pressure resulted in the condensation of water onto the sample.

Thioflavin-T measurements

Aliquots (5 μL) of insulin solutions were taken during incubation, diluted with 995 μL of 10 mM Na_2H/NaH_2PO_4, 150 mM NaCl, and 50 μM thioflavin-T solution, and stirred for 30 s. Using a Varian Cary Eclipse fluorescence spectrophotometer (Varian, Walton-on-Thames, UK), fluorescence emission intensity at 482 nm (5 nm slit width) was then measured for 30 s, exciting at 440 nm (5-nm slit width). Data was collected at small time intervals until the fluorescence appeared to have reached the ''plateau region'' (Jarrett and Lansbury, 1993), with further timepoints taken up to 24 h of incubation. Data from at least three separate experiments were averaged and normalized on a scale from 0 to 1.

UV/Vis kinetic measurements

Sheet linear polarization filters (Comar Instruments, Cambridge, UK) in perpendicular orientations were inserted on either side of the sample. At 600 nm the crossed polarization filters showed least transmission and therefore all measurements were made at this wavelength. Samples of insulin solutions were heated to 65°C (as checked inside the cuvette using a thermocouple) in glass cuvettes without stirring. Absorbance measurements were taken at 30-s intervals for the duration of the experiment. At least three separate experiments were performed before averaging the data. Data were normalized on a scale from 0 to 1.

RESULTS

Structural characterization

Incubation of solutions containing 1 mM bovine insulin at pH 2 and at temperatures of 37°C or 65°C has been shown to

result in the formation of spherulites, composed largely of radially oriented amyloid fibrils (Krebs et al., 2004). It is known that changes in the ionic strength of the solution can alter the rates of aggregation significantly (Nielsen et al., 2001b). The addition of salts, including NaCl, LiCl, NaI, $Na_3C_6H_5O_7$ (sodium citrate), and $MgCl_2$, to an ionic strength of 0.1 M resulted in the formation of spherulites with diameters apparently smaller than those formed in the absence of salts. In the case of 0.1 M NaCl, spherulite diameters of up to ~60 μm, with an average size of 20 ± 10 μm (standard deviation) were observed. In the absence of salt, spherulite diameters of up to ~140 μm, with an average size of 45 ± 25 μm (standard deviation), were observed (Fig. 1). More significantly, in the absence of salt the spherulites displayed a marked core at their centers; this core was up to 53 ± 11% of the diameter. In the presence of 0.1 M NaCl this core appeared to be significantly smaller at 12 ± 5% of the diameter (Figs. 1 and 2). At the ionic strength used (0.1 M), these observations applied regardless of the atomic radius and charge of the cation or anion added. This suggests that this effect can be investigated using a single salt only. Therefore, all subsequent experiments were performed using NaCl as the salt.

To confirm that spherulites grown in the presence of salt contained amyloid fibrils, as do spherulites grown in the absence of salt (Krebs et al., 2004), the spherulites were imaged by confocal microscopy using thioflavin-T as the fluorescent dye. Thioflavin-T is a dye whose fluorescence intensity increases markedly upon binding to amyloid fibrils (LeVine, 1993; Naiki et al., 1989). In transmission mode and under crossed polars, images from spherulites formed in the presence and absence of NaCl demonstrate the Maltese cross, as observed by optical microscopy (Figs. 1 and 3). Confocal images of spherulites grown in the presence or absence of salt appeared indistinguishable from each other and clearly show that thioflavin-T is associated preferentially with the spherulites (Fig. 3). This suggests that they contain amyloid fibrils, supporting conclusions drawn earlier (Krebs et al., 2004). The confocal images also display a non-fluorescent core in the spherulites, which could be due to nonpenetration of the dye. As this core is present even after incubating the spherulites in the presence of the dye for several hours, however, a more likely reason for its presence is the absence of significant amounts of amyloid material in the core. The fluorescence intensity in the confocal images is not always evenly distributed across a spherulite (Fig. 3), as a consequence of the regular orientation of the fibrils and the regular association of thioflavin-T with the dye. Further analysis of this observation has allowed us to describe a likely binding site for the dye on the amyloid fibrils (Krebs et al., 2005).

Inserting a waveplate at a 45° angle to the crossed polars in an optical microscope allows the determination of the orientation of the amyloid fibrils within the spherulites. Spherulites grown in the presence of NaCl showed the same optical pattern as that described for spherulites formed in the absence of NaCl (Krebs et al., 2004) (see Supplementary Material), suggesting that the fibrils are oriented radially in the spherulites.

The radial arrangement of amyloid fibrils in the spherulites can be observed directly and more clearly when examining the spherulite structures by ESEM. ESEM allows imaging of soft or biological structures without the prior need for dehydration (Donald, 2003). A drop of solution containing spherulites is applied to a sample stub and inserted into the microscope chamber. Maintaining the sample at 2°C and the chamber pressure at ~5 Torr, the vapor pressure of water at 2°C, the hydration state of the sample can be controlled. A decrease in pressure below ~5 Torr leads to evaporation and drying of the sample; conversely, an increase in pressure will result in the condensation of more water on the sample (Donald, 2003). Initially, no spherulites can be observed when a drop of a spherulite-containing solution is imaged in the microscope. Reducing the chamber pressure slowly results in surface water being removed from the sample, and spherulites appear as spherical objects, with diameters

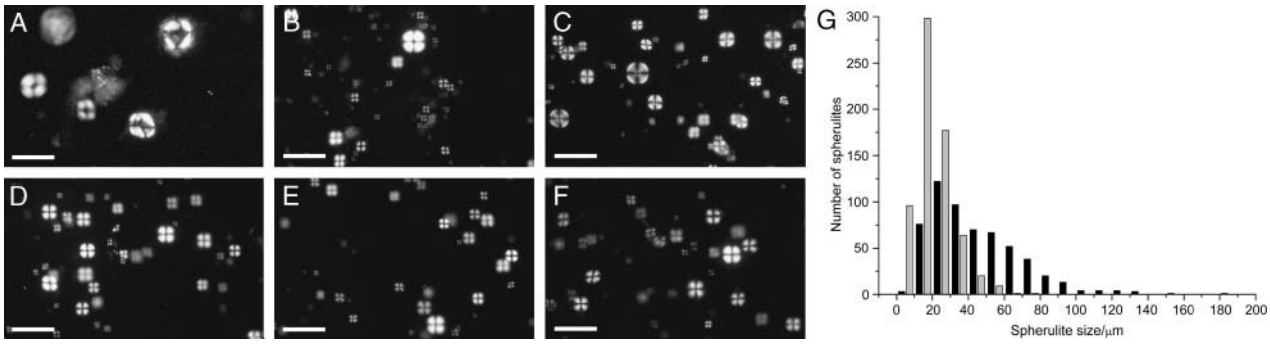

FIGURE 1 Insulin amyloid spherulites formed in the presence of various salts. Optical microscopy images of solutions of 1 mM insulin, incubated at pH 2 and 65°C for 24 h. (*A*) No added salt. (*B–F*) Solutions of 0.1 M ionic strength using (*B*) NaCl, (*C*) NaI, (*D*) $Na_3C_6H_5O_7$ (sodium citrate), (*E*) $MgCl_2$, and (*F*) LiCl. Scale bar in all pictures, 100 μm. (*G*) Histogram of spherulite diameters, $n = 575$ in the absence of NaCl (*black bars*), $n = 666$ in the presence of 100 mM (*shaded bars*).

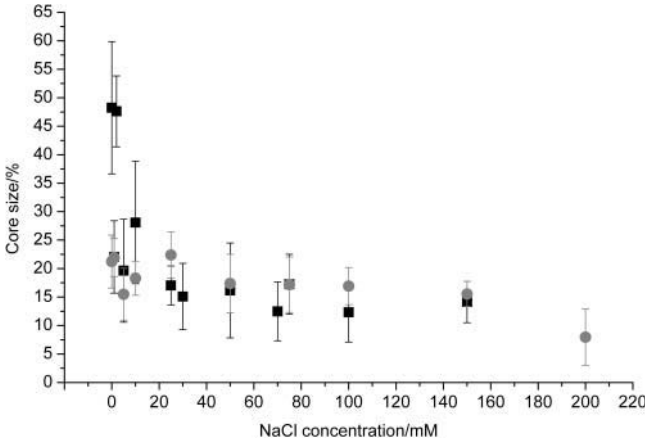

FIGURE 2 Core size at different NaCl concentrations and temperature. Core size as a percentage of spherulite diameter shown for spherulites formed by incubation of 1-mM insulin solutions at pH 2, with the indicated NaCl concentration and 65°C (*black squares*) and 55°C (*shaded circles*) for 24 h. Error bars are ± SD, based on a minimum of 30 measurements on several samples.

corresponding to those observed by optical microscopy. By further reduction of the pressure, the spherulites reduce in size as they are dehydrated, and ultimately fracture (Krebs et al., 2004). Some of the fractured spherulites reveal their interior, allowing a study of their internal structure (Fig. 4). The spherulites, whether grown in the presence or absence of

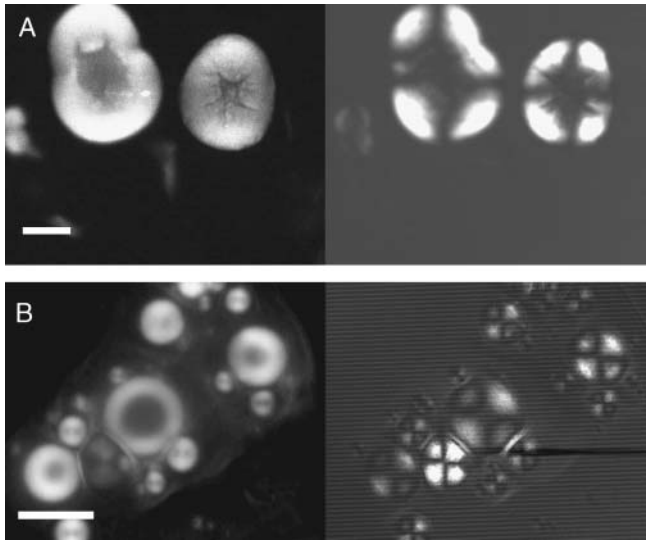

FIGURE 3 Confocal microscope analysis of insulin spherulites. Images of aliquots of solutions containing spherulites, formed by incubating 1 mM insulin at pH 2.0 and 65°C in the absence (*A*) and presence (*B*) of 100 mM NaCl. (*A*, *left*) Fluorescence confocal image, using ThT. The fluorescence is preferentially associated with those areas of the solution corresponding to spherulites, indicating the presence of amyloid fibrils in the spherulites. (*Right*) Same image as on left but in transmission mode using crossed polarizing filters. Maltese crosses indicating spherulites can clearly be seen. In *B*, the same images are shown of spherulites formed in the presence of 100 mM NaCl. Scale bar, 20 μm.

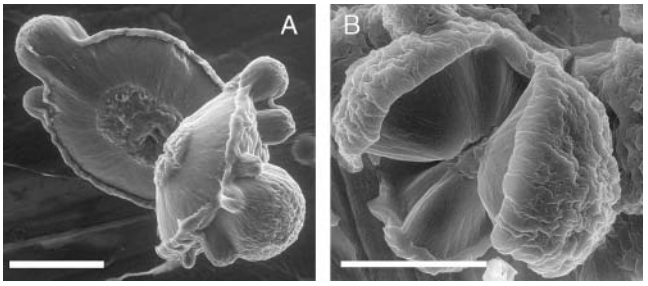

FIGURE 4 ESEM images of insulin spherulites. (*A*) Insulin spherulite formed by incubating 1 mM insulin at pH 2 and 65°C for 24 h. After rapid dehydration in the ESEM chamber, the spherulite shown has cracked and opened up, showing radial lines from the periphery to the center. The latter is not apparently regularly organized. (*B*) Insulin spherulite formed by incubation of 1 mM insulin at pH 2 and 65°C in the presence of 0.1 M NaCl for 24 h. Again the rapid dehydration has caused the spherulite to open and reveal radial lines. An apparently nonregular core can be seen at the center of the spherulite. The core is substantially smaller than that observed in *A*. Scale bar in both images, 30 μm.

salt, clearly show three apparently distinct regions. In the center, a core of irregularly oriented material is observed in the ESEM. The apparent lack of fibrillar or regularly packed material at the center shown in the ESEM results in this region of the spherulites being nonbirefringent and therefore appearing as dark in optical and confocal microscopy (cf. Fig. 1). Surrounding the core is a ''corona'' of material displaying radial lines. These lines are likely to be a consequence of the radially oriented amyloid fibrils, contained in this part of the spherulites. Finally, the outer surface of the spherulites is irregular and occasionally ''folds over'' onto the interior. This is likely to be due to a combination of amyloid fibrils sticking out of the spherulites and folding over upon water evaporation, together with amyloid fibrils that were initially in solution and deposited onto the amyloid fibrils during evaporation.

Mechanistic characterization

To probe the mechanism by which spherulites form, the formation of amyloid fibrils and that of spherulites were monitored using separate techniques. As these techniques used different apparatus, this could not be done simultaneously on one sample. Solutions previously incubated showed that the spherulites in them will sink to the bottom of the sample vial. As this process takes several hours, however, this is unlikely to interfere with our kinetic measurements. Amyloid fibril formation was followed by the fluorescence of thioflavin-T (Naiki et al., 1991). Spherulite formation was followed by modifying a UV/Vis spectrometer. Crossed polarizers were inserted in the beam on either side of the sample. In the absence of spherulites, no light was transmitted to the detector, leading to a ''high absorbance''. As spherulites formed and increased in number, the sample became increasingly birefringent, resulting in light

coming through the second polarizer, and thus the absorbance decreased. Both sets of measurements were normalized on a scale from 0, corresponding to the initial state, to 1, when each assay had reached an end-value.

In the absence of salt (Fig. 5), the spherulite kinetic assay suggests the presence of spherulites from ~40 to 45 min. At these times, however, no spherulites or other birefringent species could be detected by polarized light microscopy. Indeed, amyloid fibrils, which form an integral part of the spherulites, were seen to form only after ~50–55 min. These observations therefore suggest that the apparent onset of spherulites at ~40–45 min is due to light scattering from other species in solution. ESEM showed the solution contained apparently amorphous aggregates at ~45 min. These aggregates scatter light, however, due to their amorphous nature, and would not be spherulitic or birefringent. It is thought that these aggregates become the irregular core that is found at the center of the spherulites by serving as nucleation sites for fibril growth.

In the presence of salt, the kinetics were appreciably different (Fig. 6), as has been observed before (Nielsen et al., 2001b). Fibril formation started after a lag phase of only a few minutes, whereas scattering did not start until at least 20 to 25 min had passed. As before, no spherulites could be observed by optical microscopy at 20 to 25 min, so the increase in the ''spherulite'' signal is again likely due to scattering from the amorphous aggregates that have formed in solution.

The kinetics of fibril formation were similar to those considered typical of amyloid fibrils, consisting of a lag phase, a growth phase, and a plateau region (Jarrett and Lansbury, 1993). During the lag phase, a nucleus is formed that is elongated during the growth phase until no further growth occurs, resulting in the plateau region (Jarrett and

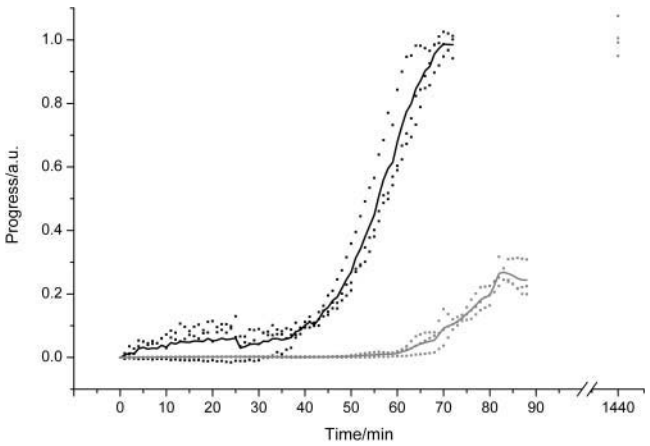

FIGURE 5 Kinetics of fibril and spherulite formation in the absence of NaCl. Samples of 1 mM insulin were incubated at pH 2 and 65°C. Thick lines show the average kinetics, squares the spread of the data for fibril formation (*shaded*) and spherulite formation (*black*). An additional fibril kinetics time point taken at 24 h is also shown. The presence of spherulites was confirmed by optical microscopy after each experiment.

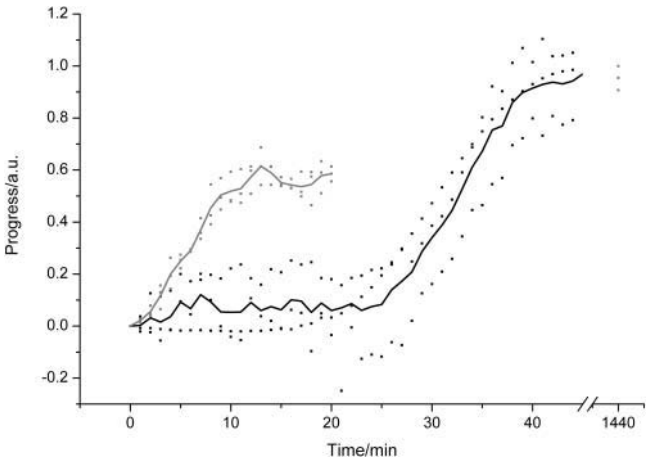

FIGURE 6 Kinetics of fibril and spherulite formation in the presence of 0.1 M NaCl. Samples of 1 mM insulin and 0.1 M NaCl were incubated at pH 2 and 65°C. Lines show the average kinetics, squares the spread of the data for fibril formation (*shaded*) and spherulite formation (*black*). An additional fibril kinetics time point taken at 24 h is also shown. Samples were checked by optical microscopy to confirm the presence of spherulites at the end of each experiment.

Lansbury, 1993). It is interesting to note that, even though an apparent plateau region had been reached after ~90 min in the absence and after ~15 min in the presence of salt, not all protein was converted into aggregates at this stage. Indeed, the thioflavin-T fluorescence intensity continued to rise, albeit more slowly than during the growth phase, until a maximum value was reached after 18–24 h (Figs. 5 and 6). After this amount of time, 90 ± 3% of the protein in the absence of salt (Krebs et al., 2004) and 95 ± 4% of the protein in the presence of salt is converted into fibrils and spherulites, denoting an end to the aggregation. The kinetics of spherulite formation take on a shape similar to those for fibril formation (Figs. 5 and 6). It has been suggested that systems that display this type of kinetics all have a similar mechanism underlying them (Jarrett and Lansbury, 1993). For fibrils, the nature of the nucleus is still widely debated and uncertain (Kelly, 2000). In the case of spherulites, the nonregular core at the heart of the spherulites is likely to form the nucleus. This irregular and therefore nonbirefringent structure, which could give rise to the observation of an apparent spherulite signal in the spherulite assay before spherulites could be detected by optical microscopy, is likely to have formed by a process of random aggregation. These data therefore suggest that fibril formation and random aggregation occur concurrently under the conditions described here. Amyloid fibrils nucleate both in solution and, if present, on the cores formed by random aggregation. The fibrils nucleated on this core will elongate outwards from the core, resulting ultimately in the formation of spherulites. It is therefore the relative rates of fibril formation and random aggregation that determine the structural details of the spherulites observed.

DISCUSSION

To form amyloid fibrils, proteins need to be in a partially folded state (Uversky and Fink, 2004). In a partially folded state, however, several different pathways are open to the protein, including refolding and aggregation. The relative populations of the different states will depend on the conditions, thermodynamics, and kinetics of any particular system (Dobson, 2003). The simultaneous occurrence of random aggregation and amyloid fibril formation has been observed before (Khurana et al., 2001; Zurdo et al., 2001). Furthermore, nucleation of fibrils on apparently irregular cores has also been observed (Blackley et al., 2000; Zhu et al., 2002). Indeed, the balance between random aggregation and ordered fibril formation plays a major role in the formation of amyloid fibrils (Chiti et al., 1999; Dobson, 2003). Under the conditions described, low pH and elevated temperatures, insulin is known to adopt a partially folded conformational state (Bouchard et al., 2000; Hua and Weiss, 2004; Nielsen et al., 2001b). The presence of two pathways, fibril formation and random aggregation, to the partially folded protein state offers an explanation for the different spherulite and core sizes observed when solutions of insulin are incubated in the absence or presence of salt. In the absence of salt, initially only random aggregation occurs, suggesting that this is the faster process. When amyloid fibrils start to form at later times, not all will form from a nucleus in solution; some will nucleate on the cores that have already formed by random aggregation. These cores will have grown to substantial sizes, giving rise to large spherulites with cores representing a significant proportion of their total volume. Addition of salt will result in the shielding of charge and therefore faster formation both of amyloid fibrils (Nielsen et al., 2001b) and of random aggregation. A similar effect of salt on aggregation kinetics has also been described for the SH3 domain (Zurdo et al., 2001). Compared to the insulin aggregation rates in the absence of salt, the rates of both fibril formation and random aggregation are enhanced. The rate of fibril formation, however, would appear to be enhanced much more substantially than that of random aggregation, and fibril formation precedes random aggregation. Once random aggregation starts occurring, fibrils can nucleate onto them very efficiently and thus form spherulites with much smaller cores than observed in the absence of salt. Furthermore, more rather than bigger cores will form, therefore resulting in the formation of more and smaller spherulites. These effects can be seen when comparing Fig. 1, *A* and *B*.

The origins of the changing kinetics of fibril formation and random aggregation are not well understood, but must be intimately involved with the mechanisms underlying both processes (Dobson, 2003; Khurana et al., 2001; Nielsen et al., 2001a,b; Zurdo et al., 2001). Amyloid fibril formation depends on a partial unfolding of the native protein (Dobson, 2003; Fändrich et al., 2003; Uversky and Fink, 2004; Zurdo et al., 2001). Indeed, aggregation rates and morphologies of fibrillar and other aggregates formed by insulin were found to change when the incubation conditions were changed either by alterations in the concentration of guanidine or by changes in the nature or concentration of added salts (Ahmad et al., 2003; Nielsen et al., 2001b). The different stability, association state, and compactness, consequences of the changes in solution conditions, were thought to be responsible for the observed changes in the aggregates formed after incubation (Ahmad et al., 2003; Nielsen et al., 2001b).

The notion that fibril formation and random aggregation occur concurrently, ultimately leading to the formation of spherulites, allows the formulation of several predictions. First and most obviously, solutions should contain both amyloid fibrils and spherulites. This has indeed been shown by wet-mode atomic force microscopy (AFM), which showed amyloid fibrils and objects too large and soft to be imaged by AFM (not shown). Optical microscopy on aliquots from the same solutions showed the presence of spherulites. Furthermore, the model predicts that the size of the core should depend on the concentration of salt used. The addition of NaCl alters the relative rates of fibril and random aggregate formation, and as the NaCl concentration increases, rates increase and the size of the core should decrease. This is indeed observed (Fig. 2). A different way of influencing the rates of fibril and random aggregate formation is by maintaining the protein in a more folded state. Experiments have shown that fibril formation is most efficient when proteins are partially folded; upon further unfolding, random aggregation occurs more readily than fibril formation (Fändrich et al., 2003; Zurdo et al., 2001). By lowering the incubation temperature for solutions of insulin, fibril formation should be favored over random aggregation, and spherulites with smaller core sizes should be observed. At low concentrations of salt, incubation of solutions of insulin at 55°C does indeed result in spherulites with smaller core sizes when compared to samples incubated at 65°C (Fig. 2). At salt concentrations above ~30 mM the core sizes of spherulites formed at both temperatures are roughly equal, as the screening of charge by the salt will result in an acceleration of random aggregation.

A final prediction based on this model is perhaps more subtle. In certain peptide systems, the formation of spherulites has been shown to be reversible (Aggeli et al., 2001, 2003). This was attributed to their formation being the consequence of a solution containing amyloid fibrils undergoing a phase transition from an isotropic solution to a solution with a continuous isotropic phase containing anisotropic droplets (Aggeli et al., 2001, 2003). A similar mechanism of spherulite formation by phase transition is likely to be responsible for that observed in crystallizing proteins, where no unfolding is occurring (Chow et al., 2002; Coleman et al., 1960; Tanaka et al., 1997), in chitin (Murray and Neville, 1998), and in DNA (Rill, 1986). Some of these systems were furthermore shown to form solutions containing continuous anisotropic

phases at higher concentrations (Aggeli et al., 2001, 2003; Revol and Marchessault, 1993; Rill, 1986). The spherulites under investigation here, however, form by fibrils nucleating on a core and are therefore more similar to irreversible aggregates. Although this could be described as a form of phase separation, the resulting structures are different from those observed in the peptide system (Aggeli et al., 2001, 2003) and exhibit none of their phase behavior. Indeed, taking solutions containing spherulites and reducing their volume (by centrifugation and removal of the supernatant), and subsequently reincubating the solutions at 65°C for 48 h did not result in the formation of a continuous anisotropic phase. Similarly, starting with fresh insulin solutions at concentrations of up to 10 mM resulted in the formation of spherulites, and continuous anisotropic phases were not observed (not shown). Therefore the reversibility observed in the peptide system (Aggeli et al., 2001, 2003) is not apparently present in the insulin system described here.

Incubating natively folded proteins under conditions where the native structure is perturbed will result in several pathways being open to the protein, including amyloid fibril formation and random aggregation (Dobson, 2003). The degree of destabilization greatly influences the rates at which various structures can form (Fändrich et al., 2003; Zurdo et al., 2001). These rates are intimately connected with the amino acid sequence of the protein, in effect altering the propensity of the polypeptide chain to form different aggregates (Dobson, 2003). Therefore, although other proteins could form spherulites under partially denaturing conditions, the rates at which they do so, and the morphology of the spherulites formed, could vary considerably from those observed here. β-lactoglobulin, for example, forms spherulites that appear to contain significantly smaller cores and form far less readily than do insulin spherulites (Bromley et al., 2004; Sagis et al., 2002).

Finally, the simultaneous occurrence of fibril formation and random aggregation leading to the formation of spherulites, can be likened to the mechanisms proposed to lead to the formation of spherulites of polyethylene (Bassett, 2003; Magill, 2001). Lamellae are composed of regularly folded polymer chains, which are nucleated either by chains starting folding or on the surface of already existing lamellae. While lamellae form, other chains can remain between lamellae in a disordered state (Bassett, 2003; Magill, 2001). The occurrence of both regularly packed material and randomly oriented material is similar to the mechanism proposed for the formation of insulin spherulites. This agrees with the notion that polypeptide chains, once beyond biological control, behave similarly to synthetic polymers (Krebs et al., 2004).

CONCLUSIONS

The structure of spherulites, formed by incubating 1 mM bovine insulin solutions with ionic strength of 0.1 M at pH 2 and 65°C for 24 h has been shown to be largely similar to the structure of spherulites formed in the absence of salt. At the center of the spherulites, a nonbirefringent core of apparently disordered material is observed. The addition of salt results in a significant reduction of the size of this core. Confocal microscopy using ThT, an amyloid fibril-specific dye, reveals the presence of amyloid fibrils in spherulites, whether formed in the presence or absence of salt. Under the polarized light microscope, addition of a full waveplate to the optical set-up showed that spherulites grown in the absence or presence of salt contain radially oriented amyloid fibrils. Observations made by ESEM agree with these conclusions.

The different effect the addition of NaCl has on the rates of fibril formation and of spherulite formation, suggests that fibril formation and random aggregation, leading to formation of the irregular core observed at the heart of spherulites, occur simultaneously but with different kinetics. Fibrils will nucleate in solution and also on randomly aggregated cores. In the latter case the fibrils grow outwards from the surface of the random aggregates resulting in the formation of spherulites. Therefore, the relative rates of fibril formation and random aggregation will determine the size of spherulites and the size of their core. Solutions containing spherulites are indeed found to contain amyloid fibrils as well. A dependence of the core size on the salt concentration is similarly predicted and found. The effect of lowering the temperature will be to favor fibril formation over random aggregation, resulting in spherulites with smaller core sizes. The proposed mechanism of spherulite formation is unlike that observed for DNA and short peptides, and the rich phase behavior those systems display has not been observed in the case of insulin spherulites. Finally, the simultaneous formation of regularly ordered and disordered material is not dissimilar to the formation of regular lamellae as well as inclusion of nonfolded polyethylene chains in polyethylene spherulites. Thus proteins that are no longer under biological control can exhibit behavior similar to that commonly attributed to synthetic polymers.

SUPPLEMENTARY MATERIAL

An online supplement to this article can be found by visiting BJ Online at http://www.biophysj.org.

The authors thank Dr. Jamie Hobbs for help with the AFM experiments and two anonymous reviewers for constructive criticism and suggestions.

The authors acknowledge the Engineering and Physical Sciences Research Council for funding M.R.H.K. and the Biotechnology and Biological Sciences Research Council for funding S.S.R. E.H.C.B. is funded by an Medical Research Council Discipline Hopper grant.

REFERENCES

Acebo, E., M. Mayorga, and J. F. Val-Bernal. 1999. Primary amyloid tumor (amyloidoma) of the jejunum with spheroid type of amyloid. *Pathol.* 31:8–11.

Aggeli, A., M. Bell, L. M. Carrick, C. W. G. Fishwick, R. Harding, P. J. Mawer, S. E. Radford, A. E. Strong, and N. Boden. 2003. pH as a trigger of peptide β-sheet self-assembly and reversible switching between nematic and isotropic phases. *J. Am. Chem. Soc.* 125:9619–9628.

Aggeli, A., G. Fytas, D. Vlassopoulos, T. C. B. McLeish, P. J. Mawer, and N. Boden. 2001. Structure and dynamics of self-assembling β-sheet peptide tapes by dynamic light scattering. *Biomacromolecules.* 2:378–388.

Ahmad, A., I. S. Millett, S. Doniach, V. N. Uversky, and A. L. Fink. 2003. Partially folded intermediates in insulin fibrillation. *Biochemistry.* 42:11404–11416.

Bassett, D. C. 2003. Polymer spherulites: a modern assessment. *J. Macromol. Sci. Phys.* 42:227–256.

Blackley, H. K. L., G. H. W. Sanders, M. C. Davies, C. J. Roberts, S. J. B. Tendler, and M. J. Wilkinson. 2000. In-situ atomic force microscopy study of β-amyloid fibrillization. *J. Mol. Biol.* 298:833–840.

Bouchard, M., J. Zurdo, E. J. Nettleton, C. M. Dobson, and C. V. Robinson. 2000. Formation of insulin amyloid fibrils followed by FTIR simultaneously with CD and electron microscopy. *Protein Sci.* 9:1960–1967.

Bromley, E. H. C., M. R. H. Krebs, and A. M. Donald. 2005. Aggregation across the length-scales in β-lactoglobulin. *Faraday Discuss.* 128:13–27.

Chiti, F., P. Webster, N. Taddei, A. Clark, M. Stefani, G. Ramponi, and C. M. Dobson. 1999. Designing conditions for in vitro formation of amyloid protofilaments and fibrils. *Proc. Natl. Acad. Sci. USA.* 96:3590–3594.

Chow, P. S., J. Zhang, X. Y. Liu, and R. B. H. Tan. 2002. Spherulitic growth in protein solutions. *Int. J. Mod. Phys. B.* 16:354–358.

Coleman, J. E., B. J. Allan, and B. L. Vallee. 1960. Protein spherulites. *Science.* 131:350–352.

Dobson, C. M. 2003. Protein folding and misfolding. *Nature.* 426:884–890.

Donald, A. M. 2003. The use of environmental scanning electron microscopy for imaging wet and insulating materials. *Nat. Mater.* 2:511–515.

Donald, A. M., and A. H. Windle. 1992. Liquid Crystalline Polymers. Cambridge University Press, Cambridge, UK.

Fändrich, M., V. Forge, K. Buder, M. Kittler, C. M. Dobson, and S. Diekmann. 2003. Myoglobin forms amyloid fibrils by association of unfolded polypeptide segments. *Proc. Natl. Acad. Sci. USA.* 100:15463–15468.

Fezoui, Y., D. M. Hartley, D. M. Walsh, D. J. Selkoe, J. J. Osterhout, and D. B. Teplow. 2000. A de novo designed helix-turn-helix peptide forms nontoxic amyloid fibrils. *Nat. Struct. Biol.* 7:1095–1099.

Gránásy, L., T. Pusztai, T. Börzsöny, J. A. Warren, and J. F. Douglas. 2004. A general mechanism of polycrystalline growth. *Nat. Mater.* 3:645–650.

Hofrichter, J. 1986. Kinetics of sickle hemoglobin polymerization. III. Nucleation rates determined from stochastic fluctuations in polymerization progress curves. *J. Mol. Biol.* 189:553–571.

Hua, Q.-X., and M. A. Weiss. 2004. Mechanism of insulin fibrillation. *J. Biol. Chem.* 279:21449–21460.

Jarrett, J. T., and P. T. J. Lansbury. 1993. Seeding ''one-dimensional crystallization'' of amyloid: a pathogenic mechanism in Alzheimer's disease and scrapie? *Cell.* 73:1055–1058.

Jin, L.-W., K. A. Claborn, M. Kurimoto, M. A. Geday, I. Maezawa, F. Sohraby, M. Estrada, W. Kaminsky, and B. Kahr. 2003. Imaging linear birefringence and dichroism in cerebral amyloid pathologies. *Proc. Natl. Acad. Sci. USA.* 100:15294–15298.

Kelly, J. W. 2000. Mechanisms of amyloidogenesis. *Nat. Struct. Biol.* 7:824–826.

Khurana, R., J. R. Gillespie, A. Talapatra, L. J. Minert, C. Ionescu-Zanethi, I. Millett, and A. L. Fink. 2001. Partially folded intermediates as critical precursors of light chain amyloid fibrils and amorphous aggregates. *Biochemistry.* 40:3525–3535.

Kobayashi, S., L. J. Hobson, J. Sakamoto, S. Kimura, J. Sugiyama, T. Imai, and T. Itoh. 2000. Formation and structure of artificial cellulose spherulites via enzymatic polymerization. *Biomacromolecules.* 1:168–173.

Krebs, M. R. H., E. H. C. Bromley, and A. M. Donald. 2005. The binding of thioflavin-T to amyloid fibrils: localization and implications. *J. Struct. Biol.* 149:30–37.

Krebs, M. R. H., C. E. MacPhee, A. F. Miller, I. Dunlop, C. M. Dobson, and A. M. Donald. 2004. The formation of spherulites by amyloid fibrils of bovine insulin. *Proc. Natl. Acad. Sci. USA.* 101:14420–14424.

LeVine III, H. 1993. Thioflavine T interaction with synthetic Alzheimer's disease β-amyloid peptides: detection of amyloid aggregation in solution. *Protein Sci.* 2:404–410.

Lockwood, N. A., R. van Tankeren, and K. H. Mayo. 2002. Aqueous gel formation of a synthetic peptide derived from the β-sheet domain of platelet factor-4. *Biomacromolecules.* 3:1225–1232.

MacPhee, C. E., and C. M. Dobson. 2000. Formation of mixed fibrils demonstrates the generic nature and potential utility of amyloid nanostructures. *J. Am. Chem. Soc.* 122:12707–12713.

Magill, J. H. 2001. Spherulites: a personal perspective. *J. Mater. Sci.* 36: 3143–3164.

Manuelidis, L., W. Fritch, and Y.-G. Xi. 1997. Evolution of a strain of CJD that induces BSE-like plaques. *Science.* 277:94–98.

Murray, S. B., and A. C. Neville. 1997. The role of the electrostatic coat in the formation of cholesteric liquid crystal spherulites from α-chitin. *Int. J. Biol. Macromol.* 20:123–130.

Murray, S. B., and A. C. Neville. 1998. The role of pH, temperature and nucleation in the formation of cholesteric liquid crystal spherulites from chitin and chitosan. *Int. J. Biol. Macromol.* 22:137–144.

Naiki, H., K. Higuchi, M. Hosokawa, and T. Takeda. 1989. Fluorometric determination of amyloid fibrils in vitro using the fluorescent dye, *Thioflavine T*. *Anal. Biochem.* 177:244–249.

Naiki, H., K. Higuchi, K. Nakakuchi, and T. Takeda. 1991. Kinetic analysis of amyloid fibril polymerization in vitro. *Lab. Invest.* 65:104–110.

Nielsen, L., S. Frokjaer, J. Brange, V. N. Uversky, and A. L. Fink. 2001a. Probing the mechanism of insulin fibril formation with insulin mutants. *Biochemistry.* 40:8397–8409.

Nielsen, L., R. Khurana, A. Coats, S. Frokjaer, J. Brange, S. Vyas, V. N. Uversky, and A. L. Fink. 2001b. Effect of environmental factors on the kinetics of insulin fibril formation: elucidation of the molecular mechanism. *Biochemistry.* 40:6036–6046.

Olson, R. A. 1970. Microtubular spherulites: development and growth in solutions of bacteriochlorophyll protein. *Science.* 169:81–82.

Raffen, R., L. J. Dieckman, M. Szpunar, C. Wunschl, P. R. Pokkuluri, P. Dave, D. Wilkins-Stevens, X. Cai, M. Schiffer, and F. J. Stevens. 1999. Physicochemical consequences of amino acid variations that contribute to fibril formation by immunoglobulin light chains. *Protein Sci.* 8:509–517.

Revol, J.-F., and R. H. Marchessault. 1993. In vitro chiral nematic ordering of chitin crystallites. *Int. J. Biol. Macromol.* 15:329–335.

Rill, R. L. 1986. Liquid crystalline phases in concentrated aqueous solutions of Na^+ DNA. *Proc. Natl. Acad. Sci. USA.* 83:342–346.

Ring, S. G., M. J. Miles, V. J. Morris, R. Turner, and P. Colonna. 1987. Spherulitic crystallization of short chain amylose. *Int. J. Biol. Macromol.* 9:158–160.

Ruth, L., D. Eisenberg, and E. F. Neufeld. 2000. α-L-Iduronidase forms semi-crystalline spherulites with amyloid-like properties. *Acta Crystallogr.* D56:524–528.

Sagis, L. M. C., C. Veerman, R. Ganzevles, M. Ramaekers, S. G. Bolder, and E. van der Linden. 2002. Mesoscopic structure and viscoelastic properties of β-lactoglobulin gels at low pH and low ionic strength. *Food Hydrocoll.* 16:207–213.

Sipe, J. D. 1992. Amyloidosis. *Annu. Rev. Biochem.* 61:947–975.

Snow, A. D., R. Sekiguchi, D. Nochlin, P. Fraser, K. Kimata, A. Mizutani, M. Arai, W. A. Schreier, and D. G. Morgan. 1994. An important role of heparan sulfate proteoglycan (perlecan) in a model system for the deposition and persistence of fibrillar Aβ-amyloid in rat brain. *Neuron.* 12:219–234.

Sunde, M., and C. C. F. Blake. 1997. The structure of amyloid fibrils by electron microscopy and x-ray diffraction. *Adv. Protein Chem.* 50: 123–159.

Tanaka, S., M. Yamamoto, K. Ito, R. Hayakawa, and M. Ataka. 1997. Relation between the phase separation and the crystallization in protein solutions. *Phys. Rev. E.* 56:R67–R69.

Taniyama, H., A. Kitamura, Y. Kagawa, K. Hirayama, T. Yoshino, and S. Kamiya. 2000. Localized amyloidosis in canine mammary tumors. *Vet. Pathol.* 37:104–107.

Uversky, V. N., and A. L. Fink. 2004. Conformational constraints for amyloid fibrillation: the importance of being unfolded. *Biochim. Biophys. Acta.* 1698:131–153.

Vos, J. H., and E. Gruys. 1985. Amyloid in canine mammary tumors. *Vet. Pathol.* 22:347–354.

Waugh, D. F. 1946. A fibrous modification of insulin. *J. Am. Chem. Soc.* 68:247–250.

Westlind-Danielsson, A., and G. Arnerup. 2001. Spontaneous in vitro formation of supramolecular β-amyloid structures, ''βamy balls'' by amyloid 1–40 peptide. *Biochemistry.* 40:14736–14743.

Zhu, M., P. O. Souillac, C. Ionescu-Zanetti, S. A. Carter, and A. L. Fink. 2002. Surface-catalyzed amyloid fibril formation. *J. Biol. Chem.* 277: 50914–50922.

Zurdo, J., J. I. Guijarro, J. L. Jiménez, H. R. Saibil, and C. M. Dobson. 2001. Dependence of solution conditions of aggregation and amyloid formation by an SH3 domain. *J. Mol. Biol.* 311:325–340.